J Mol Model (2010) 16:235–241
DOI 10.1007/s00894-009-0539-5

ORIGINAL PAPER

Density functional computational studies on (E)-2-[(2-Hydroxy-5-nitrophenyl)-iminiomethyl]-4-nitrophenolate

Hasan Tanak · Metin Yavuz

Received: 18 March 2009 / Accepted: 6 May 2009 / Published online: 3 July 2009

Abstract Density functional calculations of the structure, atomic charges, molecular electrostatic potential and thermodynamic functions have been performed at B3LYP/6-31G(d,p) level of theory for the title compound (E)-2-[(2-hydroxy-5-nitrophenyl)-iminiomethyl]-4-nitrophenolate. The results show that the phenolate oxygen atom and all of the nitro group oxygen atoms have bigger negative charges, and the coordination ability of these atoms differs in different solvents. The energetic behavior of the title compound in solvent media has been examined using B3LYP method with the 6-31G(d,p) basis set by applying the Onsager method and the isodensity polarized continuum model (IPCM). The results obtained with these methods reveal that the IPCM method yielded a more stable structure than Onsager's method. In addition, natural bond orbital and frontier molecular orbital analysis of the title compound were performed using the B3LYP/6-31G(d,p) method.

Keywords Schiff base · Density functional theory · Molecular electrostatic potential · Solvent effect · Natural bond orbital

Introduction

Schiff bases and their complexes are of great interest in many fields of chemistry and biochemistry because of their versatile metal binding ability [1, 2]. Moreover, Schiff bases also have biological activities such as antimicrobial [3, 4], antifungal [5], antitumor [6, 7] activities, and herbicidal properties [8]. On the industrial scale, they have a wide range of applications, such as in dyes and pigments [9]. Schiff base compounds display interesting photochromic and thermochromic features in the solid state and can be classified in terms of these properties [10]. Photo- and thermo-chromism arise via H-atom transfer from the hydroxy O atom to the N atom [11, 12]. Such proton-exchanging materials can be utilized for the design of various molecular electronic devices [13]. In general, Schiff bases display two possible tautomeric forms, the phenol-imine (OH) and the keto-amine (NH) forms. Depending on the tautomers, two types of intramolecular hydrogen bonds are observed in Schiff bases: O–H···N in phenol-imine [14, 15] and N–H···O in keto-amine [16–18] tautomers. Another form of Schiff base compounds known as zwitterion has an ionic intramolecular hydrogen bond (N^{+}–H···O^{-}); this form is rarely seen in the solid state [19–22]. The NH form of Schiff bases in the solid state can be regarded as a resonance hybrid of two canonical structures, i.e., the NH and zwitterionic forms [22].

Investigations into the structural stability of these compounds using both experimental techniques and theoretical methods have been of interest for many years. With recent advances in computer hardware and software, it is possible to correctly describe the physico-chemical properties of molecules from first principles by various computational techniques [23]. In recent years, density functional theory (DFT) has been a shooting star in theoretical modeling. The development of ever better exchange-correlation functionals has made it possible to calculate many molecular properties with accuracies comparable to those of traditional correlated ab initio methods, with more favorable computational costs [24].

H. Tanak (✉) · M. Yavuz
Department of Physics, Faculty of Arts and Sciences,
Ondokuz Mayıs University,
Kurupelit 55139 Samsun, Turkey
e-mail: htanak@omu.edu.tr

Literature surveys have revealed the high degree of accuracy of DFT methods in reproducing the experimental values in terms of geometry, dipol moment, vibrational frequency, etc. [25–31].

The X-ray crystal structure of (E)-2-[(2-hydroxy-5-nitrophenyl)-iminiomethyl]-4-nitrophenolate has already been discussed [32]; to the best of our knowledge, no theoretical calculation on this compound has yet been published. In this work, we have investigated the energetic and structural properties of (E)-2-[(2-hydroxy-5-nitrophenyl)-iminiomethyl]-4-nitrophenolate in gas phase and in solvent media, using DFT calculations.

Computational details

DFT calculations with a hybrid functional B3LYP (Becke's three parameter hybrid functional using the LYP correlation functional) at 6-31G(d,p) basis set using the Berny method [33, 34] were performed with the Gaussian 03 software package [35], and Gauss-view visualization program [36]. The calculated vibrational frequencies verified that the structures were stable (no imaginary frequencies).

In order to evaluate the energetic and atomic charge behavior of the title compound in solvent media, we carried out theoretical calculations in the five kinds of solvent (ε= 78.39, H_2O; ε=46.7, DMSO; ε=24.55, C_2H_5OH; ε=10.36, CH_2ClCH_2Cl; ε=4.9, $CHCl_3$). The methodologies used in this investigation are centered on two solvation methods: Onsager's reaction field theory [37] of electrostatic solvation, and the isodensity polarized continuum model (IPCM) [38].

To investigate the reactive sites of the title compound, the molecular electrostatic potential (MEP) was evaluated using B3LYP/6-31G(d,p) method. The MEP, $V(r)$, at a given point $r(x,y,z)$ in the vicinity of a molecule, is defined in terms of the interaction energy between the electrical charge generated from the molecule electrons and nuclei and a positive test charge (a proton) located at r. For the system studied, $V(r)$ values were calculated as described previously using Eq. 1 [39],

$$V(r) = \sum Z_A/|R_A - r| - \int \rho(r')/|r' - r| d^3 r' \qquad (1)$$

where Z_A is the charge of nucleus A, located at R_A, $\rho(r')$ is the electronic density function of the molecule, and r' is the dummy integration variable.

The thermodynamic properties of the title compound at different temperatures were calculated on the basis of vibrational analyses. In addition, natural bond orbital (NBO) and frontier molecular orbitals (FMO) were performed with B3LYP/6-31G(d,p) on the optimized structure.

Results and discussion

Geometrical structure

The crystal structure of the title compound is monoclinic, and the space group is P21/c. The crystal structure parameters of the title compound are a=7.9649 (1) Å, b= 8.6110 (1) Å, c=19.1190 (3) Å, β=98.433 (2) ° and V= 1,297.11 (3) $Å^3$ [32].

DFT calculations of the title compound were performed at B3LYP/6-31G(d,p) level of theory. Some optimized parameters (bond lengths) are also shown in Fig. 1b. The molecular structure of the title compound shown in Fig. 1a is nearly planar. According to X-ray studies [32], the dihedral angle between the C1/C6 and C8/C13 rings is 178.42 (16)°, whereas the dihedral angle has been calculated at −179.99° for B3LYP . When the X-ray structure of the title compound is compared with its optimized counterpart (see Fig. 1b), conformational discrepancies between the two can be observed.

The most notable discrepancy exists in the orientation of the N1–H1N bond, which has an intramolecular N1–H1N···O1 hydrogen bond. For the N1–H1N···O1 hydrogen bond that exists between the phenolate O1 atom and imine N1 atom, D-H, H···A and D-H···A values are 0.94(4) Å, 1.72(4) Å, 156(3)° for X-ray [32] and 1.05 Å, 1.671 Å, 140.48° for B3LYP, respectively. Another difference in the optimized structure is observed in the relative orientation of each of the nitro groups. Each of the nitro oxygen atoms is twisted slightly out of the plane of the molecule [torsion angles = 172.16 (17)° (O3–N2–C4–C5); −7.1 (2)° (O4–N2–C4–C5); −7.6 (3)° (O3–N2–C4–C3); 173.17 (15)° (O4–N2–C4–C3); and 178.63 (16)° (O6–N3–C12–C13); −3.4 (3)° (O5–N3–C12–C13); 174.28 (18)° (O5–N3–C12–C11); −3.7 (3)° (O6–N3–C12–C11)] [32]. These torsion angles have been calculated at −179.99917°, −0.00214°, 0.00147°, 179.9985° and 179.99785°, 0.00035°, 180.0°, −0.00251° for B3LYP/6-31G(d,p) level, respectively.

As seen from Fig. 1, most of the optimized bond lengths are slightly longer than the experimental values. We noted that the experimental results belong to the solid phase and theoretical calculations belong to the gas phase. In the solid state, the existence of the crystal field along with the intermolecular interactions has connected the molecules together, which results in differences in bond parameters between calculated and experimental values. The biggest difference in bond lengths occurs mainly in the group involved in the hydrogen bond [i.e., N1–C7], which can be easily understood by taking into account the intramolecular hydrogen bond interactions present in the crystal.

In spite of the differences observed, the calculated geometric parameters are, in general, in good agreement with the X-ray structure [32]. Based on the optimized

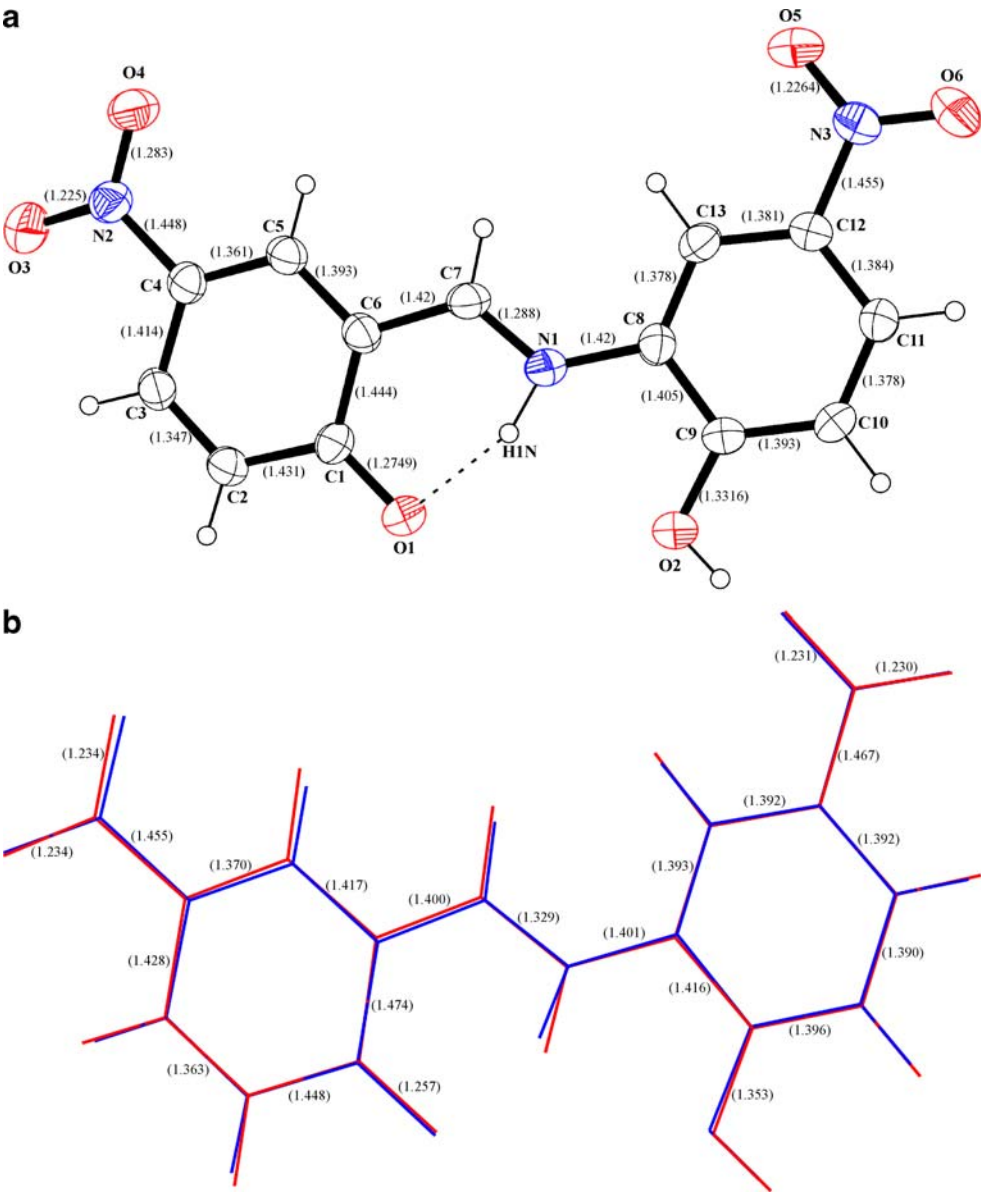

Fig. 1 **a** Experimental geometrical structure and bond lengths of the title compound (E)-2-[(2-hydroxy-5-nitrophenyl)-iminiomethyl]-4-nitrophenolate [32]. **b** Atom-by-atom superimposition of the calculated structure (*red*) over the X-ray structure (*blue*) for the title compound and calculated bond lengths

geometry, atomic charge distribution, MEP, NBO, FMO and thermodynamic properties of the title compound are discussed as follows.

Atomic charge distributions in gas phase and in solution phase

The Mulliken atomic charges and natural population analysis (NPA) atomic charges for the non-H atoms of the title compound were calculated at B3LYP/6-31G(d,p) level in gas phase. In addition, to investigate the solvent effect for the atomic charge distributions of the title compound, based on the B3LYP/6-31G(d,p) model and the Onsager model, three kinds of solvent (ε=78.39, H_2O; ε=24.55, C_2H_5OH; ε=4.9, $CHCl_3$) were selected. The Mulliken and NPA atomic charges shows that the O1 atom and nitro group oxygen atoms (O3 and O4) have bigger negative atomic charges [−0.594927e (Mulliken)/−0.63555e (NPA) for O1, −0.405812e (Mulliken)/−0.39424e (NPA) for O3 and −0.416270e (Mulliken)/−0.40282e (NPA) for O4], calculated at B3LYP/6-31G(d,p) level in gas phase. This behavior can be the result of electronegativity of the nitro group and intramolecular N1-H1N···O1 hydrogen bond. On the other hand, it could be that in solution-phase, the atomic charge values of the nitro group oxygen atoms are bigger than those in gas-phase, and while their atomic charge values increase with the increase of the polarity of the solvent with values −0.429143e (ε=4.9), −0.444235e (ε=24.55) and −0.448020e (ε=78.39) for O3 and −0.436265e (ε=4.9), −0.446662e (ε=24.55) and −0.449102e (ε=78.39) for O4 atom, the value of O1 decreases with the increase in solvent polarity, with values −0.579891e (ε=4.9),

−0.572257e (ε=24.55) and −0.570477e (ε=78.39). This result reveals that the coordination ability of O1 atom and nitro group oxygen atoms will differ in different solvents, which may be helpful if one wants to use the title compound to construct interesting metal complexes with different coordinate geometries [40].

In order to evaluate the energetic behavior of the title compound in solvent media, we carried out calculations in five kinds of solvent (ε=78.39, H_2O; ε=46.7, DMSO; ε=24.55, C_2H_5OH; ε=10.36, CH_2ClCH_2Cl; ε=4.9, $CHCl_3$). Total energies and dipole moments were calculated in solvent media at B3LYP/6-31G (d,p) level using Onsager and IPCM models and the results are presented in Table 1.

According to Table 1, we can conclude that the total energies of the title compound obtained by Onsager and IPCM methods decrease with the increasing polarity of the solvent, while the stability of the title compound increases in going from the gas phase to the solution phase. The energy difference between the gas phase and solvent media is given in Fig. 2 for both methods. As can be seen from Fig. 2, the IPCM method provided a more stable structure than Onsager's method (22 kcal mol^{-1} on average).

NBO analysis

NBO analysis provides an efficient method for studying intra- and inter-molecular bonding and interaction among bonds, and also provides a convenient basis for investigating charge transfer or conjugative interaction in molecular systems [41]. The larger the $E^{(2)}$ value, the more intensive is the interaction between electron donors and electron acceptors, i.e., the more donating tendency from electron donors to electron acceptors and the greater the extent of conjugation of the whole system. Delocalization of electron density between occupied Lewis-type (bond or lone pair) NBO orbitals and formally unoccupied (antibond or Rydgberg) non-Lewis NBO orbitals correspond to a stabilizing donor–acceptor interaction.

Table 1 Total energies and dipole moments of the title compound (E)-2-[(2-hydroxy-5-nitrophenyl)-iminiomethyl]-4-nitrophenolate in different solvents. *IPCM* Isodensity polarized continuum model

Method	ε[a]	Energy (a.u.)	μ (debyes)	Δ*E* (kcal/mol)[b]
B3LYP	1	−1,116.2194864	8.3040	
Onsager	4.9	−1,116.2253159	11.835	−3.65832
	10.36	−1,116.2271047	13.055	−4.78081
	24.55	−1,116.2282826	13.900	−5.51995
	46.7	−1,116.2287442	14.242	−5.80961
	78.39	−1,116.2289616	14.404	−5.94603
IPCM	4.9	−1,116.2522938	11.504	−20.582
	10.36	−1,116.2605581	12.326	−25.7731
	24.55	−1,116.2655402	12.827	−28.8994
	46.7	−1,116.2673983	13.016	−30.0654
	78.39	−1,116.268255	13.103	−30.603

[a] Dielectric constant

[b] $E_{solvation}-E_{gas}$

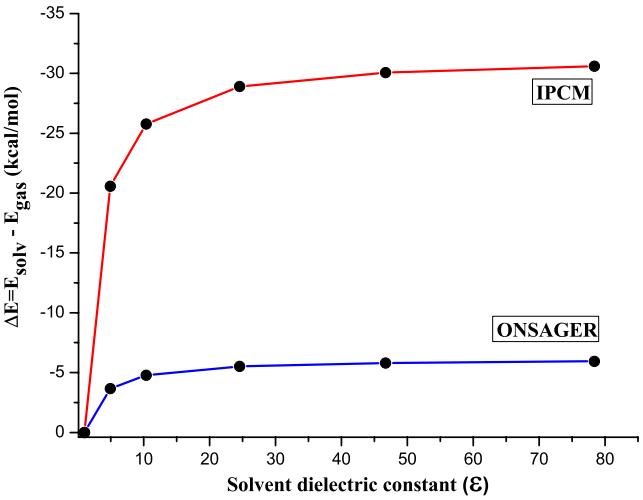

Fig. 2 Energy difference between the gas phase and solvent media by isodensity polarized continuum model (IPCM) and Onsager methods at B3LYP/6-31G(d,p) level of theory

For each donor NBO(*i*) and acceptor NBO(*j*), the stabilization energy $E^{(2)}$ associated with electron delocalization between donor and acceptor is estimated as [42, 43]

$$E^{(2)} = -q_i \frac{(F_{ij})^2}{\varepsilon_j - \varepsilon_i} \quad (2)$$

where q_i is the donor orbital occupancy, ε_i,ε_j are diagonal elements (orbital energies) and F_{ij} is the off-diagonal NBO Fock matrix element. The results of second-order perturbation theory analysis of the Fock Matrix at B3LYP/6-31G(d,p) level of theory are presented in Table 2.

NBO analysis revealed that the *n*(O1)→σ(N1–H1N) interactions give the strongest stabilization to the system of the title compound by 27 kcal mol^{-1}, and strengthen the intramolecular N1–H1N···O1 hydrogen bond. The lone pair of O1 also donates its electrons to σ-type antibonding orbital for O2–H2O. The total stabilization energy of O2–H2O···O1 intermolecular hydrogen bonding is 23.92 kcal mol^{-1}, which is quite large. The weak NBO interactions of the *n*(O3)→σ(C3–H3A), *n*(O5)→σ(C7–H7A) and *n*(O5)→σ(C13–H13A) imply the existence of C–H···O hydrogen bonds that have total stabilization energies 2.55, 4.83 and 2.93 kcal mol^{-1}, respectively. Desiraju [44] and Neuheuser et al. [45] estimated the energy of the C–H···O hydrogen bond as 1.0–2.0 and 1.2–1.8 kcal mol^{-1}, respectively. Thus, it is apparent that O–H···O and C–H···O intermolecular interactions significantly influence crystal packing in this molecule.

Table 2 Second-order perturbation theory analysis of the Fock matrix in natural bond orbital (NBO) basis, calculated at B3LYP/6-31G(d,p) level

Donor orbital (*i*)	Acceptor orbital (*j*)	ε_j-ε_i (a.u.)[a]	F_{ij} (a.u.)[b]	$E^{(2)}$ (kcal/mol)[c]
LP(1) O3	BD*(1) C3-H3A	1.30	0.041	1.63
LP(2) O3	BD*(1) C3-H3A	0.80	0.025	0.92
LP(1) O5	BD*(1) C7-H7A	1.28	0.041	1.63
LP(2) O5	BD*(1) C7-H7A	0.78	0.045	3.20
LP(1) O5	BD*(1) C13-H13A	1.29	0.042	1.70
LP(2) O5	BD*(1) C13-H13A	0.77	0.032	1.23
LP(1) O1	BD*(1) O2-H2O	1.19	0.097	9.95
LP(2) O1	BD*(1) O2-H2O	0.79	0.096	13.97
LP(1) O1	BD*(1) N1-H1N	1.04	0.073	6.28
LP(2) O1	BD*(1) N1-H1N	0.71	0.127	27.81

[a] Energy difference between donor and acceptor *i* and *j* NBO orbitals

[b] Fock matrix element between *i* and *j* NBO orbitals

[c] Energy of hyper conjugative interactions

Molecular electrostatic potential

MEP is related to the electronic density and is a very useful descriptor in understanding sites of electrophilic attack and nucleophilic reactions as well as hydrogen bonding interactions [46–48]. The electrostatic potential $V(r)$ is also well suited for analyzing processes based on the "recognition" of one molecule by another, such as in drug–receptor, and enzyme–substrate interactions, because it is through their potentials that the two species first "see" each other [49, 50].

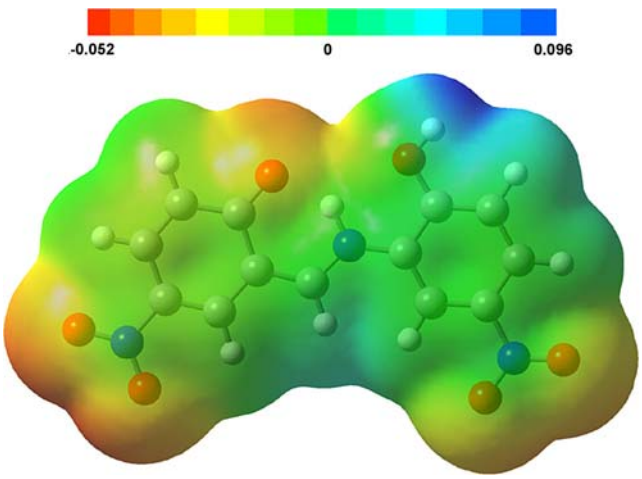

Fig. 3 Molecular electrostatic potential (MEP) map calculated at B3LYP/6-31G(d,p) level

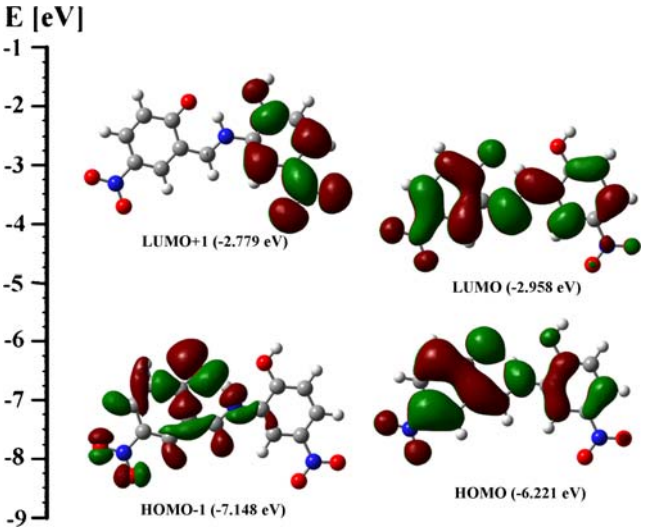

Fig. 4 Molecular orbital surfaces and energy levels given in parentheses for the HOMO−1, HOMO, LUMO and LUMO+1 of the title compound computed at B3LYP/6-31G(d,p) level

To predict reactive sites of electrophilic and nucleophilic attack for the investigated molecule, MEP at the B3LYP/6-31G(d,p) optimized geometry was calculated. The negative (red) regions of MEP were related to electrophilic reactivity and the positive (blue) regions to nucleophilic reactivity (Fig. 3). As can be seen in Fig. 3, this molecule has several possible sites of electrophilic attack. The negative regions are mainly over the oxygen atoms on each of the nitro groups and the O1 atom. The negative V(r) values are −0.052 a.u. for the region between O3 and O4 atoms, which is the most negative region: about −0.041 a.u. for the O1 atom and −0.038 a.u. for the region between O5 and O6 atoms. Thus, the calculations suggest that the preferred site for electrophilic attack is the region between O3 and O4 atoms, followed by the O1 atom. A maximum positive region is localized on the H2O atom with a

Table 3 Thermodynamic properties at different temperatures at B3LYP/6-31G(d,p) level

T (K)	$H_m^0(kcal.mol^{-1})$	$C_{p,m}^0(cal.mol^{-1}.K^{-1})$	$S_m^0(cal.mol^{-1}.K^{-1})$
200	3.76	50.14	120.90
250	6.64	60.87	133.69
298.15	9.90	70.83	145.62
300	10.04	71.20	146.07
350	13.94	80.88	158.09
400	18.31	89.74	169.75
450	23.10	97.72	181.02
500	28.27	104.84	191.90

value of +0.096 a.u. indicating a possible site of nucleophilic attack.

Frontier molecular orbitals

The FMOs play an important role in the electric and optical properties, as well as in UV-Vis spectra and chemical reactions [51]. Figure 4 shows the distributions and energy levels of the HOMO−1, HOMO, LUMO and LUMO+1 orbitals computed at the B3LYP/6-31G(d,p) level for the title compound. As seen in Fig. 4, both the highest occupied molecular orbital (HOMO) and the lowest-lying unoccupied molecular orbital (LUMO) are localized mainly in the 4-nitrophenolate fragment and nitrophenol ring as well as the N1–H1N bond. While the LUMO+1 is localized on the nitrophenol ring, the HOMO−1 is localized on the whole structure with the exception of the nitrophenol ring. The value of the energy separation between the HOMO and LUMO is 3.263 eV, and this large energy gap indicates that the title structure is very stable.

Thermodynamic properties

Based on the vibrational analysis at B3LYP/6-31G(d,p) level and statistical thermodynamics, the standard thermodynamic functions: heat capacity ($C^0_{p,m}$), entropy (S^0_m), and enthalpy (H^0_m) were obtained and listed in Table 3. The scale factor for frequencies is 0.9627 [52], which is used for an accurate prediction in determining the thermodynamic functions.

Table 3 shows that the standard heat capacities, entropies, and enthalpies increase at any temperature from 200.00 to 500.00 K, because the intensities of molecular vibration increase with increasing temperature. The correlation equations between these thermodynamic properties and temperature T are as follows:

$$C^0_{p,m} = -1.48446 + 0.28711\,T - 1.48495 \times 10^{-4}T^2\,,\left(R^2 = 0.99994\right) \quad (3)$$

$$S^0_m = 66.04035 + 0.28937\,T - 7.52779 \times 10^{-5}T^2,\left(R^2 = 1\right) \quad (4)$$

$$H^0_m = -3,41398 + 0.01717\,T + 9.25686 \times 10^{-5}T^2,\left(R^2 = 0.99997\right) \quad (5)$$

These equations will be helpful in further studies of the title compound.

Conclusions

Density functional calculations were performed for the title compound of (E)-2-[(2-Hydroxy-5-nitrophenyl)-iminiomethyl]-4-nitrophenolate and the calculated results show that the B3LYP/6-31G(d,p) method can reproduce the title compound well. The phenolate oxygen atom has a bigger negative atomic charge in gas phase, and its atomic charge value decreases with an increase in the polarity of the solvent. This result reveals that the coordination ability of the O1 atom will differ in different solvents.

The total energy of the title compound decreases with increasing polarity of the solvent, and the stability of the title compound increases in going from the gas phase to the solution phase. NBO analysis revealed that the n(O1)→σ(N1–H1N) interaction gives the strongest stabilization to the system, and the major interaction for the intermolecular O1···O2 contact is n(O1)→σ(O2–H2O). The MEP map shows several possible sites of electrophilic attack. The correlations between the thermodynamic properties $C^0_{p,m}$, S^0_m, H^0_m and temperatures T were also obtained.

References

1. Calligaris M, Randaccio L (1987) In: Wilkinson G (ed) Comprehensive coordination chemistry, vol 2. Pergamon, London, pp 715–738
2. Zhou Y-S, Zhang L-J, Zeng X-R, Vital JJ, You X-Z (2000) J Mol Struct 524:241–250
3. El-Masry AH, Fahmy HH, Abdelwahed SHA (2000) Molecules 5:1429–1438
4. Pandey SN, Sriram D, Nath G, De Clercq E (1999) Il Farmaco 54:624–628
5. Singh WM, Dash BC (1988) Pesticides 22:33–37
6. Hodnett EM, Dunn WJ (1970) J Med Chem 13:768–770
7. Desai SB, Desai PB, Desai KR (2001) Heterocycl Commun 7:83–90
8. Holla BS, Rao BS, Shridhara K, Akberali PM (2000) Il Farmaco 55:338–344
9. Taggi AE, Hafez AM, Wack H, Young B, Ferraris D, Lectka T (2002) J Am Chem Soc 124:6626–6635
10. Cohen MD, Schmidt GMJ, Flavian S (1964) J Chem Soc 2041–2051
11. Hadjoudis E, Vitterakis M, Mavridis IM (1987) Tetrahedron 43:1345–1360
12. Xu X-X, You X-Z, Sun Z-F, Wang X, Liu H-X (1994) Acta Crystallogr C50:1169–1171
13. Alarcon SH, Pagani D, Bacigalupo J, Olivieri AC (1999) J Mol Struct 475:233–240
14. Petek H, Albayrak Ç, Ağar E, Ocak İskeleli N, Şenel I (2007) Acta Cryst E63:o810–o812
15. Özek A, Albayrak Ç, Odabaşoğlu M, Büyükgüngör O (2007) Acta Cryst C63:o177–o180
16. Karabıyık H, Ocak İskeleli N, Petek H, Albayrak Ç, Ağar E (2008) J Mol Struct 873:130–136
17. Koşar B, Büyükgüngör O, Albayrak Ç, Odabaşoğlu M (2004) Acta Cryst C60:o458–o460
18. Tanak H, Erşahin F, Ağar E, Büyükgüngör O, Yavuz M (2008) Analyt Sci 24:237–238

19. Petek H, Albayrak Ç, Ocak Iskeleli N, Ağar E, Şenel I (2007) J Chem Cryst 37:285–290
20. Temel E, Albayrak Ç, Büyükgüngör O, Odabaşoğlu M (2006) Acta Cryst E62:o4484–o4486
21. Yüce S, Albayrak Ç, Odabaşoğlu M, Büyükgüngör O (2006) Acta Cryst C62:o389–o393
22. Ogawa K, Harada J (2003) J Mol Struct 647:211–216
23. Zhang Y, Guo ZJ, You XZ (2001) J Am Chem Soc 123:9378–9387
24. Proft FD, Geerlings P (2001) Chem Rev 101:1451–1464
25. Fitzgerald G, Andzelm J (1991) J Phys Chem 95:10531–10534
26. Ziegler T (1991) Pure Appl Chem 63:873–878
27. Andzelm J, Wimmer E (1992) J Chem Phys 96:1280–1303
28. Scuseria GE (1992) J Chem Phys 97:7528–7530
29. Dickson RM, Becke AD (1993) J Chem Phys 99:3898–3905
30. Johnson BG, Gill PMW, Pople JA (1993) J Chem Phys 98:5612–5626
31. Oliphant N, Bartlett RJ (1994) J Chem Phys 100:6550–6561
32. Hijji YM, Barare B, Butcher RJ, Jasinskic JP (2009) Acta Cryst E65:o291–292
33. Schlegel HB (1982) J Comput Chem 3:214–218
34. Peng C, Ayala PY, Schlegel HB, Frisch MJ (1996) J Comput Chem 17:49–56
35. Frisch MJ, Trucks GW, Schlegel HB, Scuseria GE, Robb MA, Cheeseman JR, Montgomery JA Jr, Vreven T, Kudin KN, Burant JC, Millam JM, Iyengar SS, Tomasi J, Barone V, Mennucci B, Cossi M, Scalmani G, Rega N, Petersson GA, Nakatsuji H, Hada M, Ehara M, Toyota K, Fukuda R, Hasegawa J, Ishida M, Nakajima T, Honda Y, Kitao O, Nakai H, Klene M, Li X, Knox JE, Hratchian HP, Cross JB, Bakken V, Adamo C, Jaramillo J, Gomperts R, Stratmann RE, Yazyev O, Austin AJ, Cammi R, Pomelli C, Ochterski JW, Ayala PY, Morokuma K, Voth GA, Salvador P, Dannenberg JJ, Zakrzewski VG, Dapprich S, Daniels AD, Strain MC, Farkas O, Malick DK, Rabuck AD, Raghavachari K, Foresman JB, Ortiz JV, Cui Q, Baboul AG, Clifford S, Cioslowski J, Stefanov BB, Liu G, Liashenko A, Piskorz P, Komaromi I, Martin RL, Fox DJ, Keith T, Al-Laham MA, Peng CY, Nanayakkara A, Challacombe M, Gill PMW, Johnson B, Chen W, Wong MW, Gonzalez C, Pople JA (2004) Gaussian 03, revision E.01. Gaussian Inc, Wallingford CT
36. Frisch A, Dennington R II, Keith T, Millam J, Nielsen AB, Holder AJ, Hiscocks J (2007) GaussView reference, version 4.0. Gaussian Inc, Pittsburgh
37. Onsager L (1936) J Am Chem Soc 58:1486–1493
38. Mierts S, Scrocco E, Tomasi J (1981) Chem Phys 55:117–129
39. Politzer P, Murray J (2002) Theor Chem Acc 108:134–142
40. Jian FF, Zhao PS,1 Bai ZS, Zhang L (2005) Struct Chem 16:635–639
41. Snehalatha M, Ravikumar C, Hubert Joe I, Sekar N, Jayakumar VS (2009) Spectrochim Acta A 72:654–662
42. Schwenke DW, Truhlar DG (1985) J Chem Phys 82:2418
43. Gutowski M, Chalasinski G (1993) J Chem Phys 98:4728
44. Desiraju GR (1991) Acc Chem Res 24:290–296
45. Neuheuser T, Hess BA, Reutel C, Weber E (1994) J Phys Chem 98:6459
46. Scrocco E, Tomasi J (1978) Adv Quantum Chem 11:115–121
47. Luque FJ, Lopez JM, Orozco M (2000) Theor Chem Acc 103:343–345
48. Okulik N, Jubert AH (2005) Internet Electron J Mol Des 4:17–30
49. Politzer P, Laurence PR, Jayasuriya K, McKinney J (1985) Environ Health Perspect 61:191–202
50. Scrocco E, Tomasi J (1973) Topics in current chemistry, vol 7. Springer, Berlin, p 95
51. Fleming I (1976) Frontier orbitals and organic chemical reactions. Wiley, London
52. Merrick JP, Moran D, Radom L (2007) J Phys Chem A 111:11683–11700